

Organometallic Complex Formed by an Unconventional Radical S-Adenosylmethionine Enzyme

Min Dong,^{†,‡} Masaki Horitani,^{‡,‡} Boris Dzikovski,[†] Maria-Eirini Pandelia,[§] Carsten Krebs,^{||} Jack H. Freed,[†] Brian M. Hoffman,^{*,‡} and Hening Lin^{*,†,⊥}

[†]Department of Chemistry and Chemical Biology, Cornell University, Ithaca, New York 14853, United States

[‡]Department of Chemistry, Northwestern University, Evanston, Illinois 60208, United States

[§]Department of Biochemistry, Brandeis University, Waltham, Massachusetts 02453, United States

^{||}Department of Chemistry and Department of Biochemistry and Molecular Biology, The Pennsylvania State University, University Park, Pennsylvania 16802, United States

[⊥]Howard Hughes Medical Institute, Cornell University, Ithaca, New York 14853, United States

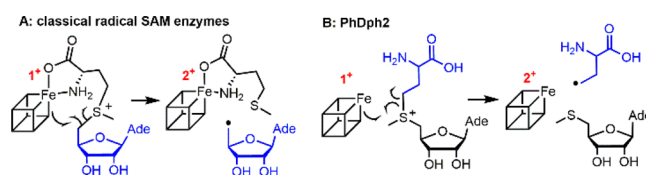
Supporting Information

ABSTRACT: *Pyrococcus horikoshii* Dph2 (*PhDph2*) is an unusual radical S-adenosylmethionine (SAM) enzyme involved in the first step of diphthamide biosynthesis. It catalyzes the reaction by cleaving SAM to generate a 3-amino-3-carboxypropyl (ACP) radical. To probe the reaction mechanism, we synthesized a SAM analogue (SAM_{CA}), in which the ACP group of SAM is replaced with a 3-carboxyallyl group. SAM_{CA} is cleaved by *PhDph2*, yielding a paramagnetic (*S* = 1/2) species, which is assigned to a complex formed between the reaction product, α -sulfinyl-3-butenoic acid, and the [4Fe-4S] cluster. Electron–nuclear double resonance (ENDOR) measurements with ¹³C and ²H isotopically labeled SAM_{CA} support a π -complex between the C=C double bond of α -sulfinyl-3-butenoic acid and the unique iron of the [4Fe-4S] cluster. This is the first example of a radical SAM-related [4Fe-4S]⁺ cluster forming an organometallic complex with an alkene, shedding additional light on the mechanism of *PhDph2* and expanding our current notions for the reactivity of [4Fe-4S] clusters in radical SAM enzymes.

Diphthamide is a post-translationally modified histidine residue on archaeal and eukaryotic translation elongation factor 2 (EF2), a protein essential for ribosomal protein synthesis. Its biosynthesis involves at least seven proteins.^{1,2} The first step involves the transfer of a 3-amino-3-carboxypropyl (ACP) group derived from S-adenosyl-L-methionine (SAM) to the histidine residue of EF2. *In vitro*, the [4Fe-4S]-containing radical SAM (RS) enzyme *PhDph2*³ or the eukaryotic Dph1-Dph2 heterodimer⁴ is sufficient for this step, with dithionite as the reducing agent. In contrast to classical RS enzymes that cleave the C_{5'},Ade–S bond of SAM to form a 5'-deoxyadenosyl radical (5'-dA[•], Scheme 1A),⁵ *PhDph2* cleaves the C₇,Met–S bond to form an ACP radical (Scheme 1B).³

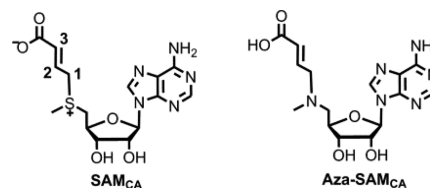
Formation of the ACP radical is supported by the *PhDph2*-catalyzed generation of 2-aminobutyric acid and homocysteine sulfinic acid in the absence of the substrate protein, *PhEF2*.³ However, the ACP radical has not been directly observed, even

Scheme 1. *PhDph2* Is Different from Classical Radical SAM Enzymes



when we carried out freeze-quench electron paramagnetic resonance (EPR) experiments (Figure S1). This is not surprising, because the ACP radical is expected to be short-lived. Following the strategy developed by Frey and co-workers to generate a more stable allylic analogue of 5'-dA[•],^{6,7} we synthesized a SAM analogue, SAM_{CA}, in which the ACP group of SAM was replaced with a 3-carboxyallyl group (Scheme 2). If

Scheme 2. Structures of SAM_{CA} and aza-SAM_{CA}



PhDph2 could accept SAM_{CA} as a substrate, a 3-carboxyallyl radical would be generated, which should be more stable and allow direct observation by EPR. As shown below, even with SAM_{CA}, we could not detect the radical intermediate. However, surprisingly, we found that a dithionite-quenched radical product formed an organometallic complex with the Fe–S cluster, revealing an interesting reactivity of the [4Fe-4S] cluster in RS enzymes.

We initially examined whether SAM_{CA} could serve as a substrate of *PhDph2*. High-performance liquid chromatography (HPLC) showed that all the SAM_{CA} was converted to 5'-deoxy-

Received: May 1, 2016

Published: July 28, 2016

5'-methylthioadenosine (MTA) within 20 min, whereas in the absence of dithionite or *PhDph2*, no SAM_{CA} was cleaved (Figure 1A). These results demonstrate that *PhDph2* is able to

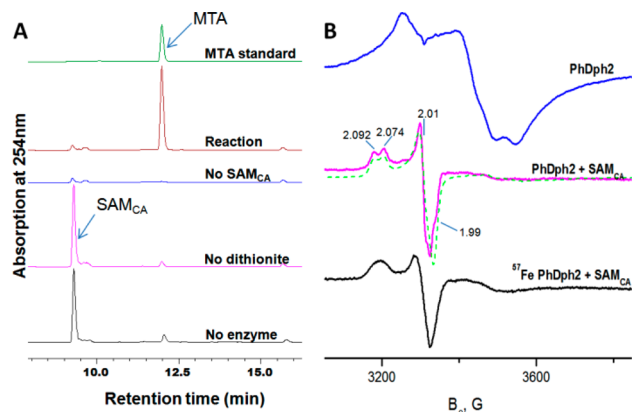


Figure 1. (A) HPLC traces of the SAM_{CA} cleavage reaction (reaction time 20 min) catalyzed by *PhDph2* at room temperature. (B) X-band CW EPR spectra of *PhDph2* in the absence and presence of SAM_{CA}. A spectral simulation for the $S = 1/2$ species is shown as green dotted line. $T = 12$ K.

catalyze the cleavage of the “correct” C–S bond of SAM_{CA}. In the presence of the substrate protein *PhEF2*, the same reaction product was detected (Figure S2). However, *PhEF2* was not modified by SAM_{CA}. This was likely because SAM_{CA} generated a more stable radical (see more experimental evidence for the stability below), which was not active enough to react with *PhEF2*.

We then prepared freeze-quench samples and used EPR to detect radical signals. The dithionite-reduced *PhDph2* in the absence of SAM_{CA} showed a typical [4Fe-4S]⁺ EPR signal at 12 K (Figure 1B),³ which was temperature-dependent and broadened beyond detection at 30 K (Figure S1). When *PhDph2* in the presence of dithionite was allowed to react with SAM_{CA} for 30 s, the [4Fe-4S]⁺ signal was replaced by a nearly axial signal, with a split feature at g_1 (Figure 1B). The ratio of this g_1 splitting at X- and Q-band scaled with the ratio of microwave frequencies (Figure S3), showing that the splitting represents two different conformations and not a hyperfine interaction with a paramagnetic nucleus. Simulation of the spectra gave for the one conformer principal g -values $g = [2.092, 2.010, 1.990]$, and for the second one $g = [2.074, 2.010, 1.990]$. Both signals exhibited similar relaxation properties and were hardly detectable above 70 K (Figure S1). The large g -anisotropy and the absence of proton hyperfine splittings suggest that it is not a free allyl radical.^{6,8} In contrast, the signals of the new species formed in the reaction of the reduced *PhDph2* with SAM_{CA} exhibited an “isotropic” g -value, $g_{\text{iso}} = (g_{11} + g_{22} + g_{33})/3 > g_e = 2.0023$,⁹ which is reminiscent of that observed in high-potential iron–sulfur proteins and [4Fe-4S]³⁺ intermediates trapped with the [4Fe-4S] proteins IspG¹⁰ and IspH.¹¹ With ⁵⁷Fe-enriched *PhDph2*, the EPR signal became broadened (Figure 1B), further supporting that the new species (termed CA) is associated with the [4Fe-4S] cluster.

When we monitored the reaction at different time points, the EPR signal of CA persisted for >30 min, even after all SAM_{CA} was consumed (Figure S4). This suggested that CA was a complex of the reaction product with the [4Fe-4S]⁺ cluster, the latter regenerated by dithionite reduction of the [4Fe-4S]²⁺

produced in the reaction. To test this hypothesis, protein-free aliquots of the reaction products were added to “fresh” dithionite-reduced *PhDph2*. An anisotropic EPR signal identical to that of CA was obtained, supporting that CA is a product complex (Figure S5).

To understand the structure of CA, we analyzed the reaction products using ¹H NMR. Several new peaks were observed from the reaction containing *PhDph2*, SAM_{CA}, and dithionite (Figure S6), which were absent in control reactions without dithionite. Some of the new peaks were assigned to MTA. Crotonic acid and its isomer, 3-butenic acid, possible hydrogen abstraction products of the carboxyallyl radical, were not formed, according to comparison to the spectra of their standards. Three new peaks (a–c) were assigned to γ -sulfinylcrotonic acid (Figure S6), and the remaining three peaks (d–f) around 5.1 and 5.8 ppm were assigned to α -sulfinyl-3-butenic acid (Figure S6); the remaining proton on α -sulfinyl-3-butenic acid is located at 3.4 ppm based on ¹H–¹H correlation spectroscopy (COSY) (Figures S14 and S15). Using 1,1-²H₂-SAM_{CA} as the substrate, peaks c, e, and f (Figure S7) disappeared, which supported the assignments. The assignments were confirmed by ¹H/¹³C heteronuclear multiple bond correlation (HMBC), heteronuclear single quantum correlation (HSQC), and ¹H–¹H COSY (Figures S8–S15). The reaction products were also chemically modified to allow detection by LC-MS (Figure S16). Our data thus demonstrated the formation of γ -sulfinylcrotonic acid and α -sulfinyl-3-butenic acid, which likely resulted from the recombination of the carboxyallyl radical with the dithionite-derived SO₂^{•-} radical, similar to previously reported reactions of radicals with dithionite.^{3,12,13} The NMR signal intensities suggested roughly equal formation of the two products.

We then performed 35 GHz continuous-wave (CW)/pulse ¹³C, ¹H, and ²H ENDOR with 1-¹³C-, 2-¹³C-, 3-¹³C-, 1,1-²H₂-, and 1,1,2,3-²H₄-labeled SAM_{CA} (see Scheme 2). Field-modulated 35 GHz CW ENDOR spectra obtained from reactions with 1-¹³C- and 2-¹³C-labeled SAM_{CA} both exhibit ¹³C doublets with broad component lines, split by the ¹³C hyperfine coupling, $A \approx 5$ –8 MHz (Figure 2). An estimate of the magnitude of the hyperfine coupling tensors for these two ¹³C sites of SAM_{CA} (Table S1) was obtained through analysis of 2D

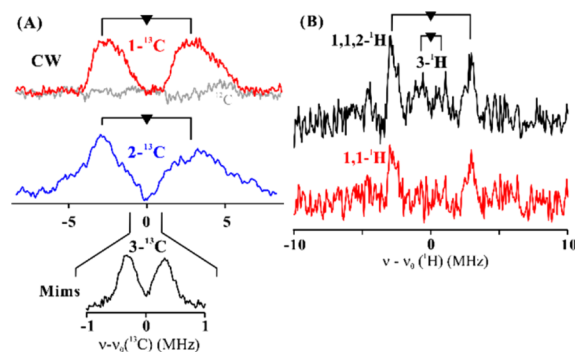


Figure 2. (A) 35 GHz CW ¹³C ENDOR spectra for CA with 1-¹³C- and 2-¹³C-labeled SAM_{CA} collected at g_2 . The doublets are split by the hyperfine coupling and centered at the Larmor frequency as described in the SI. Inset: Mims ENDOR spectra of 3-¹³C-SAM_{CA}. (B) ¹H Davies ENDOR difference spectra of CA generated by subtracting from the spectrum of ¹H-SAM_{CA} (natural abundance) the spectra for 1,1,2,3-²H-labeled SAM_{CA} (upper) and 1,1-²H-labeled SAM_{CA} (lower). Spectra were collected at g_2 and normalized by EPR echo height.

field-frequency patterns of ENDOR spectra collected across the EPR envelopes of the SAM_{CA} isotopologues (Figures S17 and S18). The analysis showed comparable isotropic hyperfine couplings, $A_{\text{iso}} \approx 7$ MHz for both $1\text{-}^{13}\text{C}$ and $2\text{-}^{13}\text{C}$. For $3\text{-}^{13}\text{C}$ -labeled SAM_{CA}, a considerably smaller isotropic coupling, $A_{\text{iso}} \approx 0.6$ MHz, was estimated using Mims pulsed ENDOR (Figure 2A, inset).

To further probe the structure of CA, ^1H and ^2H pulse ENDOR measurements were performed with $1,1\text{-}^2\text{H}_2$ - and $1,1,2,3\text{-}^2\text{H}_4$ -labeled SAM_{CA}. Only the pulsed ENDOR techniques resolved individual features, but the lower sensitivity of pulsed vs CW ENDOR allowed spectra to be collected only at the intensity maximum of the EPR envelope, near g_2 . The ^1H signals from the labeled sites were obtained by subtracting the spectra obtained using the natural-abundance SAM_{CA} (Figure 2B). After subtraction of the $1,1\text{-}^2\text{H}_2$ spectrum, a doublet of ^1H peaks assignable to the $1,1\text{-}^1\text{H}$ nuclei was obtained with coupling constant of $A \approx 7$ MHz; subtraction with the $1,1,2,3\text{-}^2\text{H}_4$ -labeled SAM_{CA} showed an enhanced intensity for this doublet (Figure 2B), indicating that the $1,1\text{-}^1\text{H}$ and $2\text{-}^1\text{H}$ nuclei had comparable couplings (assigned on the basis of $2\text{-}^{13}\text{C}$ data). In addition, weak broad features corresponding to a doublet with $A \approx 2$ MHz were assigned to $3\text{-}^1\text{H}$. Mims ^2H ENDOR spectra (Figures S19 and S20) provided support for this assignment. The substantial isotropic couplings to $1\text{-}^{13}\text{C}$ and $2\text{-}^{13}\text{C}$ ($A_{\text{iso}} \approx 7$ MHz), the deviations of the g -values from $g \approx 2$, and the ^{57}Fe broadening imply the spin is primarily localized on the cluster, but with close C–Fe interaction.

The similarity of $1\text{-}^{13}\text{C}$ and $2\text{-}^{13}\text{C}$ hyperfine couplings, as well as the similarity of the $1,1\text{-}^2\text{H}$ and the $2\text{-}^2\text{H}$ couplings, suggests that both 1-C and 2-C have similar direct interactions with the unique Fe of the $[4\text{Fe-4S}]$ cluster. In contrast, the weaker $3\text{-}^{13}\text{C}$ and $3\text{-}^2\text{H}$ hyperfine couplings show that 3-C does not experience a significant direct interaction with the Fe. These results suggest that CA consists of only one of the two products, α -sulfinyl-3-butenoic acid, coordinated to the unique Fe site of the $[4\text{Fe-4S}]$ cluster. If CA also involved a complex with γ -sulfinylcrotonic acid, 2-C and 3-C should have similar strong hyperfine couplings, and 1-C should have weaker coupling, contrary to our observations (Figure 2A). We further confirmed this by utilizing the instability of α -sulfinyl-3-butenoic acid. After the protein-free aliquots of the reaction products were incubated at room temperature overnight, the peaks corresponding to α -sulfinyl-3-butenoic acid disappeared in the ^1H NMR spectrum (Figure S21), while the signals from γ -sulfinylcrotonic acid remained. The instability of α -sulfinyl-3-butenoic acid is likely due to the acidity of the α -proton, which is adjacent to two strong electron-withdrawing groups.¹⁴ When the mixture containing only the γ -sulfinylcrotonic acid product was added to “fresh” dithionite-reduced *PhDph2*, the signal associated with CA was not detected by EPR (Figure S22). This result supports the notion that γ -sulfinylcrotonic acid does not form an EPR-active complex with the $[4\text{Fe-4S}]$ cluster and that CA is best described as a complex formed between α -sulfinyl-3-butenoic acid and the $[4\text{Fe-4S}]$ cluster.

We then probed whether the sulfinyl and carboxyl groups of α -sulfinyl-3-butenoic acid are required for CA formation. We synthesized a non-cleavable analogue of SAM_{CA}, aza-SAM_{CA} (Scheme 2).¹⁵ The freeze-quench EPR experiment with aza-SAM_{CA} showed only a $[4\text{Fe-4S}]^+$ signal (Figure S23) that was similar to that of the reduced cluster in *PhDph2* in the absence of SAM_{CA}. Therefore, CA is not formed by binding of uncleaved SAM_{CA} to the $[4\text{Fe-4S}]$ cluster. Addition of 3-

butenoic acid to *PhDph2* also failed to generate the CA species. Thus, the sulfinic group in α -sulfinyl-3-butenoic acid is likely involved in the formation of CA. Similarly, adding allylsulfonic acid to *PhDph2* did not generate the CA signal either. Thus, the carboxyl group in α -sulfinyl-3-butenoic acid is also necessary. The results suggest that both the sulfinic group and the carboxylate of α -sulfinyl-3-butenoic acid bind to the Fe–S cluster, facilitating the formation of a π -complex between that Fe and the C=C double bond of the product (Figure 3).

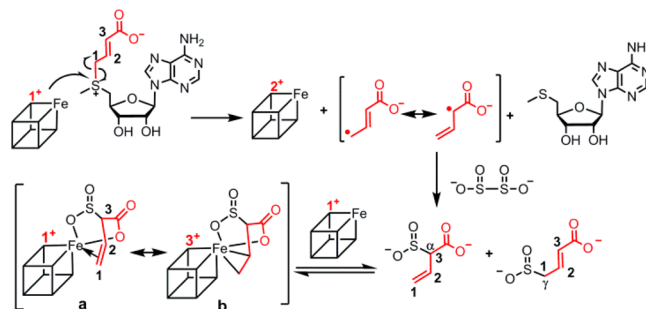


Figure 3. Plausible structures of CA and formation mechanism.

CA can have two formal resonance structures (Figure 3, structures a and b). To further probe the oxidation state of CA, we attempted to reduce CA by low-temperature γ -irradiation (cryoreduction)¹⁶ (Figure S24). The EPR signal did not decrease upon γ -irradiation, as would be expected for a $[4\text{Fe-4S}]^{3+}$ cluster. Similarly, extra dithionite could not reduce CA, which is inconsistent with the expectation for a $[4\text{Fe-4S}]^{3+}$ cluster (Figure S25).¹⁷ In contrast, when we tried to oxidize CA with $\text{K}_3[\text{Fe}(\text{CN})_6]$, CA was oxidatively degraded to a $[3\text{Fe-4S}]^+$ cluster (Figure S25), an outcome commonly observed in similar treatments of $[4\text{Fe-4S}]^+$ clusters of RS enzymes with chemical oxidants. Thus, the Fe–S core in CA behaves like a $[4\text{Fe-4S}]^+$ cluster. We also sought to use ^{57}Fe Mössbauer spectroscopy. However, owing to the rather modest yield of CA (50% of total Fe) and the presence of at least one additional EPR-silent Fe-containing product, the analysis of the spectra does not permit definitive conclusions about the electronic structure of CA (Figures S26–28).

With the characterization of reaction products and the structure of CA, we proposed a plausible mechanism for the formation of CA (Figure 3). The $[4\text{Fe-4S}]^+$ cluster in *PhDph2* provides one electron to SAM_{CA}, cleaving the C_{CA}-S bond and generating a 3-carboxyallyl radical, MTA, and a $[4\text{Fe-4S}]^{2+}$ cluster. The 3-carboxyallyl radical reacts with a dithionite-derived $\text{SO}_2^{\bullet-}$ radical, forming γ -sulfinylcrotonic acid and α -sulfinyl-3-butenoic acid. The sulfinic group, the carboxyl group, and the C=C double bond of α -sulfinyl-3-butenoic acid coordinate the $[4\text{Fe-4S}]^+$ cluster (reduced by extra dithionite) to generate the π -complex. Coordination of the sulfinic and carboxyl groups helps to place the double bond in a favorable position for π interactions with the unique Fe. The two conformers revealed by EPR (Figure 1B) could be attributed to different binding orientations of α -sulfinyl-3-butenoic acid to the $[4\text{Fe-4S}]^+$ cluster (the three chelating functional groups may exchange positions).

In summary, using SAM_{CA}, we have detected an EPR-active species, CA, formed in the enzymatic reaction of *PhDph2*. Various experiments demonstrate that CA is a complex formed between the $[4\text{Fe-4S}]^+$ cluster and one of the reaction products,

α -sulfinyl-3-butenic acid, coordinated to the unique cluster Fe through the sulfinyl and carboxylate oxygens, with the C=C double bond forming an organometallic π -complex with the Fe. Although we could not accumulate the radical intermediate that we set out to detect with SAM_{CA}, formation of both α -sulfinyl-3-butenic acid and γ -sulfinylcrotonic acid provides additional support for the radical mechanism of PhDph2 reaction, as a nucleophilic mechanism cannot account for their formation. Interestingly, although the EPR g tensor of CA shows similarity to those of [4Fe-4S]³⁺-like clusters observed in two enzymes involved in the non-mevalonate pathway, IspG and IspH, the cluster in CA behaves like a [4Fe-4S]⁺ cluster.

The present case can be described as the reaction of the unique Fe of the [4Fe-4S]⁺ cluster with the alkene product to form a stable organometallic complex. Such an alkene complex has been reported for the nitrogenase FeMo-cofactor and the ethylenic product of alkyne reduction,¹⁸ and for mutants of IspH and its substrate HMBPP.^{11,19} However, no similar organometallic complex had been demonstrated for RS enzymes until very recently, when the [4Fe-4S]²⁺ cluster of the RS enzyme, pyruvate formate-lyase activating enzyme, was shown to react with the 5'-dA• to form a highly reactive organometallic intermediate.²⁰ This study and our current result suggest that the unique iron of [4Fe-4S] clusters in RS enzymes can readily form a C-Fe complex. Such a property not only may help to explain the unusual chemistries catalyzed by the [4Fe-4S]-containing RS enzymes but also may open up new avenues to tune the activity or develop new chemistry for this enzyme class or for other [4Fe-4S]-containing enzymes.

■ ASSOCIATED CONTENT

📄 Supporting Information

The Supporting Information is available free of charge on the ACS Publications website at DOI: 10.1021/jacs.6b04155.

Experimental materials and methods, Figures S1–S36, and Tables S1 and S2 (PDF)

■ AUTHOR INFORMATION

Corresponding Authors

*bmh@northwestern.edu

*hl379@cornell.edu

Author Contributions

#M.D. and M.H. contributed equally to this work.

Notes

The authors declare no competing financial interest.

■ ACKNOWLEDGMENTS

This work is supported by NIH (GM088276, P41-GM103521, and GM111097). We thank Dr. Ivan Keresztes and Mr. Anthony Condo for assistance with NMR, and Prof. H. Halpern at University of Chicago for access to the ⁶⁰Co Gammacell irradiator.

■ REFERENCES

- (1) Su, X.; Lin, Z.; Lin, H. *Crit. Rev. Biochem. Mol. Biol.* **2013**, *48*, 515.
- (2) Schaffrath, R.; Abdel-Fattah, W.; Klassen, R.; Stark, M. J. *Mol. Microbiol.* **2014**, *94*, 1213.
- (3) Zhang, Y.; Zhu, X.; Torelli, A. T.; Lee, M.; Dzikovski, B.; Koralewski, R. M.; Wang, E.; Freed, J.; Krebs, C.; Ealick, S. E.; Lin, H. *Nature* **2010**, *465*, 891.
- (4) Dong, M.; Su, X.; Dzikovski, B.; Dando, E. E.; Zhu, X.; Du, J.; Freed, J. H.; Lin, H. *J. Am. Chem. Soc.* **2014**, *136*, 1754.

(5) Broderick, J. B.; Duffus, B. R.; Duschene, K. S.; Shepard, E. M. *Chem. Rev.* **2014**, *114*, 4229.

(6) Magnusson, O. T.; Reed, G. H.; Frey, P. A. *J. Am. Chem. Soc.* **1999**, *121*, 9764.

(7) Horitani, M.; Byer, A. S.; Shisler, K. A.; Chandra, T.; Broderick, J. B.; Hoffman, B. M. *J. Am. Chem. Soc.* **2015**, *137*, 7111.

(8) Mcmanus, H. J.; Fessenden, R. W.; Chipman, D. M. *J. Phys. Chem.* **1988**, *92*, 3778.

(9) Belinskii, M. *Chem. Phys.* **1993**, *172*, 189.

(10) Wang, W.; Li, J.; Wang, K.; Huang, C.; Zhang, Y.; Oldfield, E. *Proc. Natl. Acad. Sci. U. S. A.* **2010**, *107*, 11189.

(11) Wang, W.; Wang, K.; Span, I.; Jauch, J.; Bacher, A.; Groll, M.; Oldfield, E. *J. Am. Chem. Soc.* **2012**, *134*, 11225.

(12) Ko, Y.; Ruzsyczky, M. W.; Choi, S. H.; Liu, H. W. *Angew. Chem., Int. Ed.* **2015**, *54*, 860.

(13) Chandor-Proust, A.; Berteau, O.; Douki, T.; Gasparutto, D.; Ollagnier-de-Choudens, S.; Fontecave, M.; Atta, M. *J. Biol. Chem.* **2008**, *283*, 36361.

(14) Khatik, G. L.; Kumar, R.; Chakraborti, A. K. *Org. Lett.* **2006**, *8*, 2433.

(15) Joce, C.; Caryl, J.; Stockley, P. G.; Warriner, S.; Nelson, A. *Org. Biomol. Chem.* **2009**, *7*, 635.

(16) Davydov, R.; Hoffman, B. M. *Arch. Biochem. Biophys.* **2011**, *507*, 36.

(17) de la Torre, A.; Lara, C.; Yee, B. C.; Malkin, R.; Buchanan, B. B. *Arch. Biochem. Biophys.* **1982**, *213*, 545.

(18) Lee, H. I.; Igarashi, R. Y.; Laryukhin, M.; Doan, P. E.; Dos Santos, P. C.; Dean, D. R.; Seefeldt, L. C.; Hoffman, B. M. *J. Am. Chem. Soc.* **2004**, *126*, 9563.

(19) Wang, W.; Wang, K.; Liu, Y. L.; No, J. H.; Li, J.; Nilges, M. J.; Oldfield, E. *Proc. Natl. Acad. Sci. U. S. A.* **2010**, *107*, 4522.

(20) Horitani, M.; Shisler, K.; Broderick, W. E.; Hutcheson, R. U.; Duschene, K. S.; Marts, A. R.; Hoffman, B. M.; Broderick, J. B. *Science* **2016**, *352*, 822.